

PVA matches human liver in needle-tissue interaction

de Jong, Tonke L.; Pluymen (student), L.H.; van Gerwen, Dennis J.; Kleinrensink, GJ; Dankelman, Jenny; van den Dobbelsteen, John J.

DOI

[10.1016/j.jmbbm.2017.01.014](https://doi.org/10.1016/j.jmbbm.2017.01.014)

Publication date

2017

Document Version

Accepted author manuscript

Published in

Journal of the Mechanical Behavior of Biomedical Materials

Citation (APA)

de Jong, T. L., Pluymen (student), L. H., van Gerwen, D. J., Kleinrensink, GJ., Dankelman, J., & van den Dobbelsteen, J. J. (2017). PVA matches human liver in needle-tissue interaction. *Journal of the Mechanical Behavior of Biomedical Materials*, 69, 223-228. <https://doi.org/10.1016/j.jmbbm.2017.01.014>

Important note

To cite this publication, please use the final published version (if applicable).
Please check the document version above.

Copyright

Other than for strictly personal use, it is not permitted to download, forward or distribute the text or part of it, without the consent of the author(s) and/or copyright holder(s), unless the work is under an open content license such as Creative Commons.

Takedown policy

Please contact us and provide details if you believe this document breaches copyrights.
We will remove access to the work immediately and investigate your claim.

Short Communication

PVA Matches Human Liver in Needle-Tissue Interaction

Tonke L. de Jong^{a,+,*}, Loes H. Pluymen^{a,+}, Dennis J. van Gerwen^a, Gert-Jan Kleinrensink^b, Jenny Dankelman^a, John J. van den Dobbelsteen^b

^a*BioMechanical Engineering Department, Delft University of Technology, 2628 CD, Delft, The Netherlands*

^b*Neurosciences Department, Erasmus MC, University Medical Center, 3000CA, Rotterdam, The Netherlands*

ABSTRACT

Medical phantoms can be used to study needle-tissue interaction and to train medical residents. The purpose of this research is to study the suitability of polyvinyl alcohol (PVA) as a liver tissue mimicking material in terms of needle-tissue interaction. Insertions into ex-vivo human livers were used for reference. Six PVA samples were created by varying the mass percentage of PVA to water (4m% and 7m%) and the number of freeze-thaw cycles (1, 2 and 3 cycles, 16 hours of freezing at -19°C, 8 hours of thawing). The inner needle of an 18Gauge trocar needle with triangular tip was inserted 13 times into each of the samples, using an insertion velocity of 5mm/s. In addition, 39 insertions were performed in two ex-vivo human livers. Axial forces on the needle were captured during insertion and retraction and characterized by friction along the needle shaft, peak forces, and number of peak forces per unit length. The concentration of PVA and the number of freeze-thaw cycles both influenced the mechanical interaction between needle and specimen. Insertions into 4m% PVA phantoms with 2 freeze-thaw cycles were comparable to human liver in terms of estimated friction along the needle shaft and the number of peak forces. Therefore, these phantoms are considered to be suitable liver mimicking materials for image-guided needle interventions. The mechanical properties of PVA hydrogels can be influenced in a controlled manner by varying the concentration of PVA and the number of freeze-thaw cycles, to mimic liver tissue characteristics.

Keywords: Needle-Tissue Interaction, Medical Phantoms, Polyvinyl alcohol (PVA) hydrogel, Radiologic Liver Interventions, Tissue Mimicking Material.

1. INTRODUCTION

Medical phantoms are often used to investigate needle-tissue interaction and for training of residents in image-guided needle interventions. Studying needle-tissue interaction is important, for example, for the development of navigation models and steerable needles (e.g. (van de Berg et al., 2016)),

with which can be actively steered towards hard-to-reach lesions deep inside solid organs such as the liver. In addition, insight into needle tissue interaction is necessary for development of training phantoms for image guided interventions, which have been proved to be valuable in residents' training, in terms of improved technique, accuracy and confidence (Harvey et al., 1997).

Phantoms used in needle-tissue interaction studies and medical training simulate human tissue, and reflect different aspects of reality. In general, two phantom types can be used. The first option is the use of biological tissues; cadavers, when freshly frozen, retain most of the textural and imaging properties of human tissue (Hocking et al., 2011). However, due to practical and ethical issues, the use of biological tissues is not always a feasible option. Alternatively, tissue

+Tonke L. de Jong and Loes H. Pluymen contributed equally to this work

*Corresponding author at: BioMechanical Engineering Department of the Delft University of Technology, 2628 CD, Delft, The Netherlands (MISIT-lab, website: <http://www.misit.nl/tonke>, correspondence e-mail: T.L.deJong@tudelft.nl).

mimicking materials (TMM) are used. Such phantoms can be customized to the needs of specific research activities or training, are readily available, and in general more durable.

A significant amount of research on tissue mimicking materials has been done. A wide range of materials have been studied on their tissue mimicking properties, such as carrageenan, gellan gum, and oil-in-gelatin dispersions (Datla et al., 2014; Kuroda et al., 2005; Lazebnik et al., 2005). The current study focusses on polyvinyl alcohol (PVA), a synthetic polymer that can be crosslinked both chemically and physically, due to its comparable ultrasound imaging properties to real tissue (e.g. (Surry et al., 2004; Zell et al., 2007)).

In addition to the imaging properties, matching mechanical properties of a tissue mimicking material are essential, as organs are typically heterogeneous. For example, a liver consists of several tissue layers, such as collagenous capsule, normal functioning parenchyma and epithelial tissue, which all have their own mechanical characteristics. For this reason, tissue properties vary significantly from one location to another within the same organ (Misra et al., 2008). However, few studies have been done on the mechanical properties of PVA. Jiang et al. studied the freeze-thaw cycle number on the hydrogel structure and mechanical properties (Jiang et al., 2011), hereby focusing on the deformation of the PVA phantom, by using two high speed cameras. Additionally, the magnitude of needle insertion forces into PVA were compared with clinical force data of insertions into prostate, gathered in a different study (Podder et al., 2006). They concluded that PVA hydrogels may be suitable substitutions for soft tissues in biopsy precision research.

The aforementioned studies indicate the potential of PVA as a tissue mimicking material in terms of imaging and mechanical properties. However, due to a wide variety of materials and methods applied in previous studies, results often do not allow inter-study comparison with data on real tissue. On top of that, more research on the mechanical properties of PVA, especially needle-tissue interaction is needed, so that the heterogeneous characteristics of biological tissue can be mimicked. Therefore, the present paper combines these two points: it presents the suitability of PVA specimens in mimicking the mechanical needle reaction during insertion, by comparing it to insertions into human tissue, following the same research protocol.

Approach

The approach adopted for the current study was to insert needles into several PVA samples with variable mass percentages of PVA to water and number of freeze-thaw (FT) cycles, and characterize the forces. These forces were compared with insertion forces into ex-vivo human liver tissue.

The current study focusses on the influence of tissue

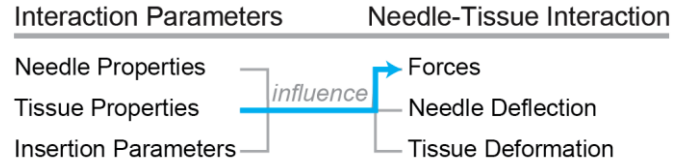


Fig. 1. Approach. Schematic depiction of the interaction parameters that influence needle-tissue interaction. In the current study, the tissue (phantom) properties are altered and the needle forces are measured (blue arrow).

(simulant) properties on the needle insertion forces. The other parameters are kept constant (Fig. 1). In addition, the data on PVA phantoms and on ex-vivo human livers are gathered using the same needle insertion parameters. In other words: the data allow for direct comparison between PVA samples and human livers.

In the present study, the axial needle force is used to characterize the mechanical interaction between needle and specimen. Forces acting on the needle can be divided in two main components, described by:

$$F_{Needle}(x) = F_{Friction}(x) + F_{tip}(x) \quad (1)$$

with F_{Needle} being the total forces acting on the needle during insertion into tissue, which are a summation of the forces that are acting on the needle tip during insertion (F_{Tip}) and forces due to friction between the needle and the surrounding tissue ($F_{Friction}$). Axial forces that act on the needle during insertion and retraction have been analyzed previously by several researchers: an extensive review of experimental data on needle-tissue interaction has been written by van Gerwen et al. (van Gerwen et al., 2012).

2. METHODS

2.1 Experimental set-up

The experimental set-up consisted of a needle and a linear motion stage holding and moving the needle (Fig. 2). An Aerotech PRO115-400 linear motion stage (Aerotech Inco, Pittsburgh, USA) was used to insert the needle into the specimen at a constant speed by moving the needle vertically with respect to specimen surface. The hub of the needle was connected with a load sensor to measure the axial forces on the needle during insertion and retraction.

The needles used during the experiments were the inner needles of 18Gauge Disposable Two-Part Trocar Needles (Cook Medical, Bloomington, USA), to eliminate the force effects of the cannula and allow for proper comparison between the PVA samples and human livers. These needles are made from stainless steel, 200mm long and have a triangular shaped tip with three facets (Fig. 3). Two-Part

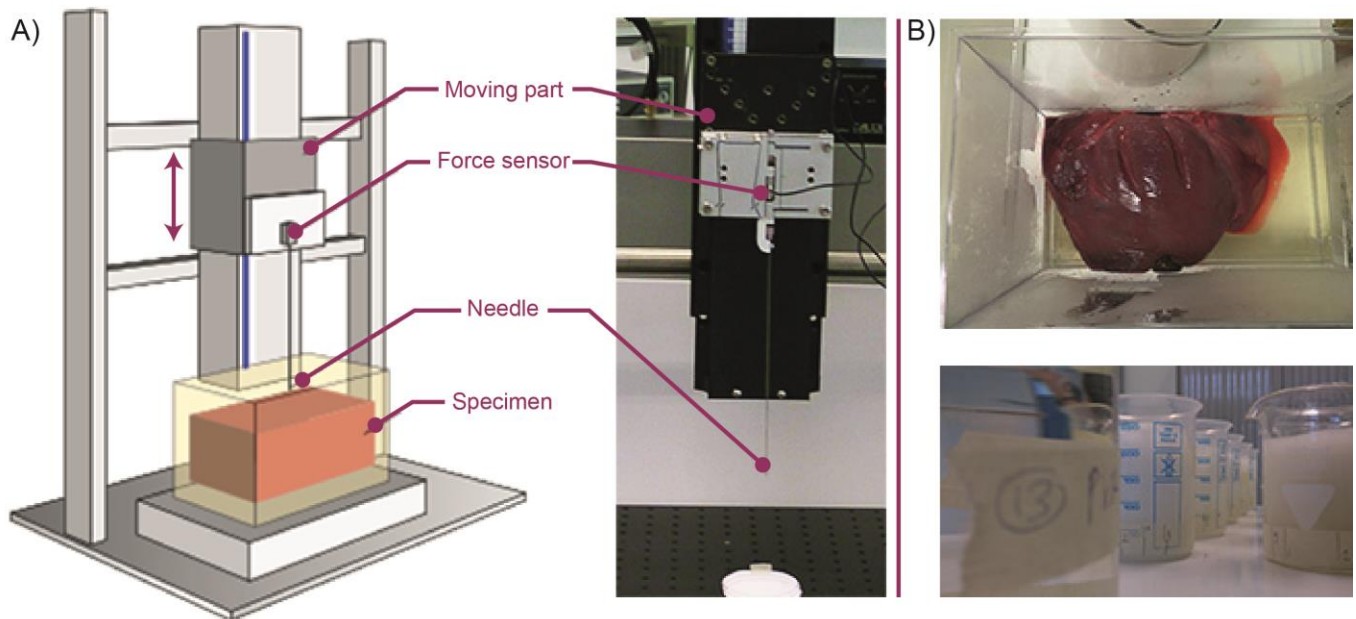


Fig. 2. Experimental set-up and specimens. A) An 18 Gauge Trocar needle was either inserted into PVA specimens, or ex-vivo human liver specimens embedded in gelatin, while the forces were measured by the load sensor. B) Above: ex-vivo liver specimen placed on a gelatin base layer. Bottom: PVA specimens

Trocar needles are commonly used in radiologic interventions.

of the gelatin. [Experiments with livers were carried out by T.L.d.J.]

2.2 Specimen preparation

Human liver

Two human liver specimens were extracted from fresh-frozen cadavers. These livers were obtained from persons without hepatic cirrhosis, as the anatomy did not show any suspicious nodules. The thickness of both livers was approximately 70mm.

The livers were embedded in 10% gelatin (Dr. Oetker, Bielefeld, Germany), to simulate the abdominal environment. Embedding in gelatin took place within one day after extraction. In the meantime, the extracted livers were stored in water in a plastic box in a refrigerator ($\pm 4^{\circ}\text{C}$). The test specimens were created by placing the livers on a gelatin base layer, to enable puncturing through the whole liver. Subsequently, the liver was submerged by a second gelatin solution, to fixate the liver. This gelatin solution was cooled down to 40°C , to prevent thermal damage of the tissue. Finally, a top gelatin layer was created. The container was stored overnight in the refrigerator to ensure proper stiffening



Fig. 3. Needle tip of the 18G Two-Part trocar needle.

PVA

Physically crosslinked PVA specimens (Selvol PVOH 165, Sekisui Chemical Group NJ, USA) were created by subjecting the samples to freeze-thaw cycles. The degree of hydrolysis is related with the ability of the polymer to form crystalline regions (Brazel and Rosen, 2012). Therefore, super hydrolyzed PVA was chosen, as optimal crosslinking by FT cycles was desired. For this specific type of super hydrolyzed PVA product, 7m% PVA to water is the maximum recommended soluble concentration.

PVA particles were added to water and magnetically stirred. After submerging of all PVA particles, the solution was heated to 93°C . This temperature was maintained for 30 minutes, after which the solution was poured into a polypropylene beaker and allowed to cool down to room temperature. Then, the specimens underwent freeze-thaw cycles of 16 hours of freezing at -19°C , followed by 8 hours of thawing at room temperature.

Two PVA production variables were varied: the concentration of PVA in water and the number of freeze-thaw cycles. This resulted in six PVA specimens: 4m% and 7m% PVA to water, subjected to 1, 2 and 3 freeze-thaw cycles. No specimen replications were used. [Experiments with PVA were carried out by L.H.P.]

2.3 Experimental Design

During each run, the needle was inserted by the linear

motion stage with a constant insertion and retraction velocity of 5mm/s. The needle insertion depth was 70mm for the PVA phantoms. In case of the livers, the needle was going from the upper gelatin layer through the liver into to the lower gelatin layer, so that the entire liver was punctured (approximate height of 70mm).

The needle insertion locations were predefined to avoid repeated insertion at the same location, and randomized. The livers were each subjected to 20 needle runs, with a mutual distance of at least 10mm. Each PVA specimen was subjected to 13 needle runs, limited by the surface area of the beaker in which the specimen was created (diameter of 60mm). In total, 3 needles were used: one for the PVA experiment and one for each liver.

For every insertion and retraction, the axial forces acting on the needle hub were stored, as well as corresponding time and positions, with a sample frequency of 1KHz. The raw dataset for the liver insertions has been made publicly available (de Jong and Van den Dobbelsteen, 2016).

2.4 Data Analysis – Mechanical Characterization

To characterize the mechanical interaction between needle and tissue, we consider three metrics: 1) the *friction* acting on the needle shaft, 2) the *magnitude of the peak forces*, and 3) the *number of peaks* per unit length during insertion. All force data were analyzed using Matlab 2015b and, prior to analysis, filtered with a zero-phase moving average filter with a window of 40 samples, to reduce noise in the signal. Force data were represented in boxplots. In order to find a “realistic” PVA specimen, realistic was defined by requiring the median of the PVA results to be within the first (Q1) and third (Q3) quarter of the liver results. This method was chosen as the data were non-normal distributed.

Friction: Fig. 4 is an example of a force-position diagram of a needle insertion into liver tissue. It is assumed that during

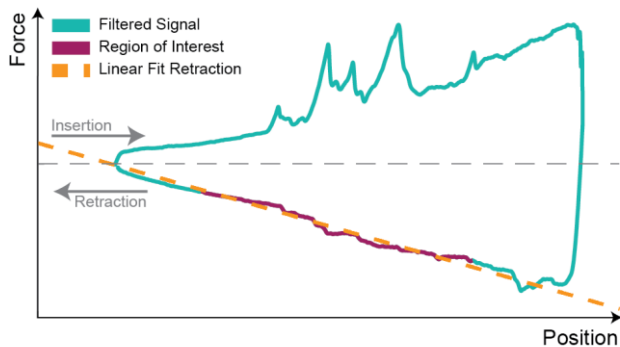


Fig. 4. Example of a force-position diagram of a needle insertion into liver tissue. The friction along the needle shaft was estimated by calculating the slope of the force during needle retraction.

needle retraction, no tip forces (F_{Tip} , see Eq. 1) are working on the needle. Previous research has shown that friction along the shaft of the instrument is approximately linearly increasing with the insertion depth (Kataoka et al., 2002). Therefore, friction can be estimated by calculating the slope during retraction of the needle, as previously done by e.g. (Hing et al., 2006; Simone, 2002).

For all needle retractions in liver and PVA specimens, a linear least squares approximation was performed. The slope of this approximation was used as an estimate for needle friction distribution along the shaft during insertion. A steeper slope, indicates more friction along the shaft of the instrument when inserted.

Peak forces – magnitude: Peaks in the force signal are typical for needle insertions into liver. Such peaks are clearly visible in the force-position diagram in Fig. 5, and may be due to encounters with inner liver structures. The magnitude of these peak forces gives information about the degree of heterogeneity of the liver.

The line simplification algorithm used in (van Gerwen et al., 2014) was selected as the classification method for the current study. This algorithm, based on the Douglas-Peucker algorithm (Douglas and Peucker, 1973), uses a single parameter, the threshold value “ ϵ ”, to extract a subset of points from the force-position curve. The threshold value represents a measure of the scale of the smallest peaks to be include, relative to the range of forces and positions measured. For the current study, a threshold value $\epsilon = 0.05$ was chosen based on visual assessment of the data. This threshold removes relatively small peaks while preserving the characteristics of the signal (Fig. 5, orange line), and thus distinguishes relevant peaks from irrelevant peaks (or noise).

Subsequently, peak height was calculated. In doing so, the signal was first corrected for overestimation, by subtracting the linear least-squares slope of the insertion phase (purple line). Then, the peak height was defined as the vertical

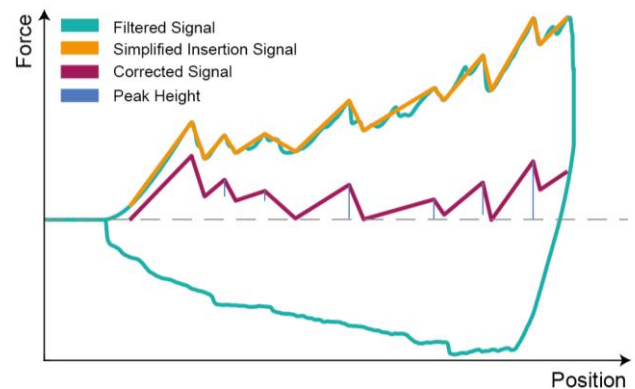


Fig. 5. Example of insertion force simplification by Douglas-Peucker algorithm and peak force analysis. First, the signal was simplified. Then, the signal was corrected for friction. For each insertion, peak heights and the number of peaks were calculated.

distance between the maximum of the corrected peak and its preceding minimum.

Peak forces - number of peaks: A third characteristic of needle insertions into tissue is the number of peaks per unit length for all insertions. This gives information on the degree of heterogeneity of the specimen. The number of peaks per unit insertion length per needle run was calculated for all insertions into PVA and compared with the insertions into liver.

3 RESULTS

Note: whereas a total of 40 insertions for the livers were planned, only 39 were taken into the analysis, due to improper saving of the force data of one needle run.

3.1 Friction

The estimated friction along the needle shaft [N/mm] can be seen in Fig. 6. The more freeze-thaw cycles, the higher the estimated friction slopes. This holds for insertions into both PVA 4m% and PVA 7m%. In addition, PVA 7m% causes higher estimated friction slopes than PVA 4m%.

The median estimated friction slope for the insertions into liver is 0.011 N/mm with the interquartile range between 0.010 N/mm and 0.013 N/mm. PVA 4m% with 2FT cycles has the same median friction slope as human liver.

The medians of the insertions into the specimens with one freeze-thaw cycle and 4m% and 7m% are respectively 0.001N/mm and 0.003N/mm, and thus below the Q1 of the liver insertions. The median estimated friction slopes of the other specimens, PVA 4m% 3FT, PVA 7m% 2FT, and PVA 7m% 3FT have a steeper friction slope than the insertions into liver.

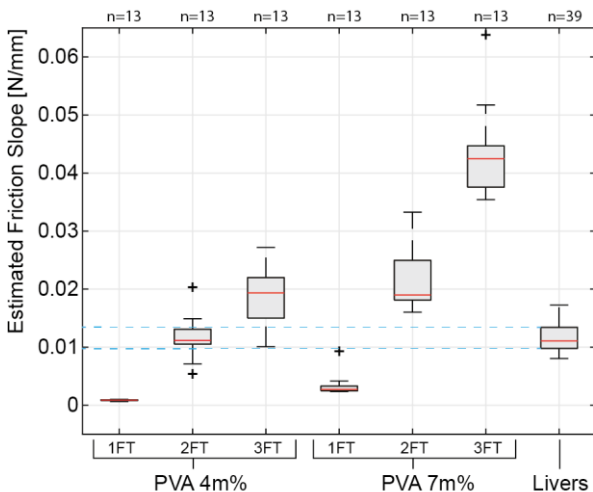


Fig. 6. Boxplot of the estimated friction slopes, i.e. the force per unit needle-specimen contact length, for needle insertions into all specimens.

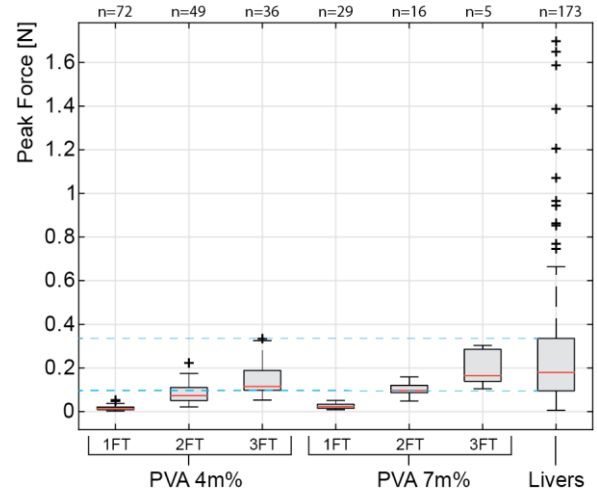


Fig. 7. Boxplot of the peak heights, calculated for all peaks found by DPA for all insertions into the specimens ($\epsilon = 0.05$).

3.2 Peak forces - magnitude

A boxplot of the magnitude of the peak forces for all insertions is shown in Fig. 7. Higher needle peak forces are found when the number of freeze-thaw cycles is increased, both for PVA 4m% and PVA 7m%. In addition, there are no striking differences in peak forces between the different specimens with the same number of freeze-thaw cycles.

Median peak forces for insertions into the PVA 4% 3FT, PVA 7m% 2FT, and PVA 7m% 3FT phantoms (respectively: 0.11N, 0.10N, and 0.16N) are all within Q1 and Q3 of the human liver specimens (median peak force = 0.18N, Q1 = 0.10N, Q3 = 0.34N), as is evident from the figure. All other specimens give rise to median needle peak forces below the interquartile range of the insertions into human livers.

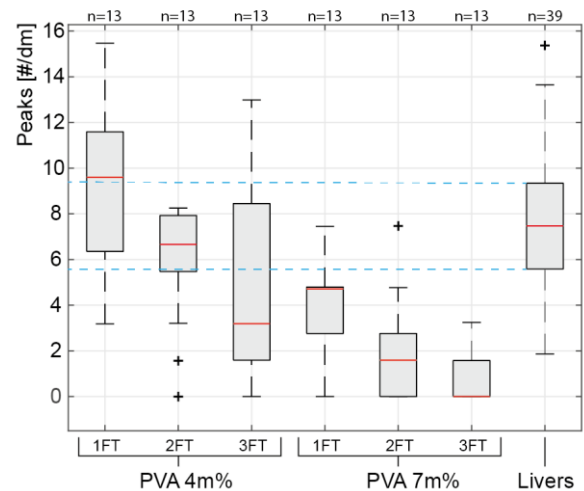


Fig. 8. Boxplot of the number of peaks per dm insertion for needle insertions into the specimens ($\epsilon = 0.05$).

3.3 Peak forces – number of peaks

Fig. 8 illustrates the number of peaks per decimeter needle insertion inside the specimen. A large range of variation can be seen for insertions into the PVA specimens and the livers, which means that the encountered number of peaks is dependent on insertion location within the specimen. An increasing number of freeze-thaw cycles causes the number of peaks to go down, which holds for both PVA concentrations. As shown in the figure, the PVA 7m% specimens have fewer peaks per unit insertion length than the PVA 4m% specimens.

The median number of peaks for insertions into liver is 7.5 per dm, with Q1 and Q3 being respectively 5.6 and 9.3 peaks per dm. PVA 4m% 2FT is the only specimen with a median that lies within Q1 and Q3 of the liver insertions (8.3 peaks per dm). The median of the number of peaks for the insertions into PVA 7m% are all below Q1 of the liver insertions.

4 DISCUSSION

In the current study, the results from needle insertions into PVA specimens were compared to those from ex-vivo human liver, in order to identify the most promising method for the production of liver mimicking phantoms in terms of mechanical reaction on the needle. Needle-tissue interaction exhibits a specific perception to the physician in radiologic needle interventions, as biological tissue is known for being mechanically heterogeneous. Therefore, it is important for a tissue simulant to imitate these heterogenic force characteristics.

PVA was chosen as a study subject, for its good tissue mimicking properties regarding ultrasound. In the present study, three mechanical force metrics were calculated and analyzed: the friction along the needle shaft during needle insertion was estimated, the magnitude of the peak forces were calculated, and the number of peak forces per unit insertion length were determined. For the estimated friction and the number of peaks per insertion length, PVA 4m% with 2FT cycles is the only specimen that is comparable with the insertions into real ex-vivo human livers. However, the magnitude of the peaks forces was most comparable for the PVA specimens that underwent 3FT cycles. In this regard, PVA 4m% with 2FT cycles falls slightly below the Q1 of the insertions into liver.

In addition to these results, the study reveals the following tendencies regarding the effect of altering the mass concentration of PVA to water and the number of freeze-thaw cycles on needle-specimen interaction:

- The friction along the needle shaft increases with an increased number of FT cycles, and with an increased mass fraction of PVA.
- The magnitude of the peaks during needle insertion increases with an increased number of FT cycles.
- The number of peak forces decreases with an increased

number of FT cycles, and with an increased mass fraction of PVA.

These trends suggest that mechanical needle-specimen interaction can be influenced in a controlled manner by altering the production variables of PVA. This is the first time, to the authors' knowledge, that these needle-tissue/phantom interactions have been compared using human livers as a reference material, subjected to the same experimental protocol as the PVA phantoms.

In general, when comparing the results of the PVA specimens with the results of the liver specimens, we see more outliers for the magnitude of the peak forces for the needle insertions into liver than for the PVA specimens (Fig 7.). In our study design, we did not plan the insertion location with respect to internal vascular structure of the liver. Therefore, we believe that these outliers might be caused by encounters of the needle with these internal structures.

On the whole, PVA 4m% with 2 freeze-thaw cycles causes the most realistic force reaction on the needle during insertion, when comparing the needle insertion force characteristics with the insertions into liver, according to the criteria defined by the present study. Median friction along the shaft of the instrument and the median number of peak forces were both within Q1 and Q3 of the insertions into the liver specimens. This indicates that PVA is a suitable liver mimicking material in terms of needle-tissue interaction.

When interpreting the results of this study, some limitations should be taken into account. First, we should note that the properties of PVA cryogels are influenced by many more variables than those that were studied in the current work. Among these are production variables and material properties, such as: the degree of hydrolysis, the degree of polymerization, the amount of ions present in the solvent, the type of solvent, and the duration of freezing and thawing (Okay and Lozinsky, 2014). We believe that making use of these PVA production variables, a specimen could be created that might be even better in mimicking our liver data set, than the PVA 4m% 2FT specimen that has been examined in this study. The published dataset of the insertions into human livers (de Jong and Van den Dobbelsteen, 2016) could be used for that purpose. Second, one should note that healthy ex-vivo human livers have been used for reference. The importance of collecting data on diseased tissue should be stressed, in addition to the current data set, as pathologic tissue is known for being stiffer and more heterogeneous (Paszek et al., 2005; Yu et al., 2011).

The present study focused on three mechanical metrics to compare the needle insertion forces in human liver and PVA phantoms, whereas an ideal liver mimicking phantom should meet requirements in other areas too. Examples include: matching imaging properties, comparable motion of the organ phantom and surrounding tissue, and similar thermal distribution after e.g. ablation procedures. The extent to which

these requirements are needed depends on the purpose of the specific medical phantom. Whereas PVA is known for its mimicking imaging properties, more research can be done to see whether the developed PVA specimens mimic other liver characteristics as well.

In short, PVA was found to be a good liver mimicking material in terms of reaction forces on the needle during insertion. A suggestion for future research includes a comparison of PVA specimens with diseased human livers. The present study can be seen as a first step in an iterative process of finding a suitable liver mimicking phantom, that can be used for training in interventional radiology.

5 CONCLUSIONS

Needle-tissue force characteristics of PVA phantoms should be studied, in addition to their imaging properties, to make realistic liver mimicking materials. Therefore, the suitability of PVA specimens for mimicking real liver tissue in terms of needle-tissue interaction was assessed. We conclude that PVA has the potential to be a realistic liver mimicking material, according to the criteria that were used in the current study. Its mechanical properties can be altered in a controlled manner by varying the production variables. These findings are relevant for the development of realistic needle insertion phantoms, which can e.g. be used for clinical training in interventional radiology and in needle-tissue interaction experiments.

ACKNOWLEDGMENT

We thank Arjan van Dijke, BioMechanical Engineering Department, Delft University of Technology, for sharing his expertise on our needle insertion set-up and for his assistance with this set-up in the hospital.

This work was supported by the Dutch Technology Foundation STW [nr. 12709].

REFERENCES

Datla, N.V., Konh, B., Koo, J.J., Choi, D.J., Yu, Y., Dicker, A.P., Podder, T.K., Darvish, K., Hutapea, P., 2014. Polyacrylamide phantom for self-actuating needle-tissue interaction studies. *Medical engineering & physics* 36, 140-145. doi: 10.1016/j.medengphy.2013.07.004

Douglas, D.H., Peucker, T.K., 1973. Algorithms for the reduction of the number of points required to represent a digitized line or its caricature. *Cartographica: The International Journal for Geographic Information and Geovisualization* 10, 112-122. doi: 10.3138/FM57-6770-U75U-7727

van Gerwen, D.J., Dankelman, J., van den Dobbelsteen, J.J., 2014. Measurement and stochastic modeling of kidney puncture forces. *Annals of biomedical engineering* 42, 685-695. doi:10.1007/s10439-013-0924-1

van Gerwen, D.J., Dankelman, J., van den Dobbelsteen, J.J., 2012. Needle-tissue interaction forces – A survey of experimental data. *Medical Engineering & Physics* 34, 665-680. doi: 10.1016/j.medengphy.2012.04.007

Yu, H., Mouw, J.K., Weaver, V.M., 2011. Forcing form and function: biomechanical regulation of tumor evolution. *Trends in Cell Biology* 21, 47-56. doi: 10.1016/j.tcb.2010.08.015

Harvey, J.A., Moran, R.E., Hamer, M.M., DeAngelis, G.A., Omary, R.A., 1997. Evaluation of a turkey-breast phantom for teaching freehand, US-guided core-needle breast biopsy. *Academic radiology* 4, 565-569. doi:10.1016/S1076-6332(97)80206-1

Hing, J.T., Brooks, A.D., Desai, J.P., 2006. Reality-based needle insertion simulation for haptic feedback in prostate brachytherapy, *Proceedings 2006 IEEE International Conference on Robotics and Automation*, 2006. ICRA 2006., pp. 619-624. doi: 10.1109/ROBOT.2006.1641779

Hocking, G., Hebard, S., Mitchell, C.H., 2011. A review of the benefits and pitfalls of phantoms in ultrasound-guided regional anesthesia. *Reg Anesth Pain Med* 36, 162-170. doi: 10.1097/AAP.0b013e31820d4207

Jiang, S., Liu, S., Feng, W., 2011. PVA hydrogel properties for biomedical application. *Journal of the Mechanical Behavior of Biomedical Materials* 4, 1228-1233. doi:10.1016/j.jmbbm.2011.04.005

de Jong, T.L., Dankelman, J., van den Dobbelsteen, J.J., 2016. Dataset of force measurements of needle insertions into two ex-vivo human livers, *Data in Brief*, "Submitted"

Kataoka, H., Washio, T., Chinzei, K., Mizuhara, K., Simone, C., Okamura, A., 2002. Measurement of the Tip and Friction Force Acting on a Needle during Penetration, in: Dohi, T., Kikinis, R. (Eds.), *Medical Image Computing and Computer-Assisted Intervention — MICCAI 2002*. Springer Berlin Heidelberg, pp. 216-223. doi: 10.1007/3-540-45786-0_27

Kuroda, M., Kato, H., Hanamoto, K., Shimamura, K., Uchida, T., Wang, Y., Akaki, S., Asaumi, J., Himeji, K., Takemoto, M., 2005. Development of a new hybrid gel phantom using carrageenan and gellan gum for visualizing three-dimensional temperature distribution during hyperthermia and radiofrequency ablation. *Int J Oncol* 27, 175-184. doi: 10.3892/ijo.27.1.175

Lazebnik, M., Madsen, E.L., Frank, G.R., Hagness, S.C., 2005. Tissue-mimicking phantom materials for narrowband and ultrawideband microwave applications. *Physics in medicine and biology* 50, 4245. doi: 10.1088/0031-9155/50/18/001

Misra, S., Reed, K.B., Douglas, A.S., Ramesh, K.T., Okamura, A.M., 2008. Needle-Tissue Interaction Forces for Bevel-Tip Steerable Needles. *Proc IEEE RAS EMBS Int Conf Biomed Robot Biomechatron*, 224-231. doi: 10.1109/BIOROB.2008.4762872

Okay, O., Lozinsky, V., 2014. *Polymeric Cryogels*. Springer. doi: 10.1007/978-3-319-05846-7

Paszek, M.J., Zahir, N., Johnson, K.R., Lakins, J.N., Rozenberg, G.I., Gefen, A., Reinhart-King, C.A., Margulies, S.S., Dembo, M., Boettiger, D., Hammer, D.A., Weaver, V.M., 2005. Tensional homeostasis and the malignant phenotype. *Cancer Cell* 8, 241-254. doi: 10.1016/j.ccr.2005.08.010

Podder, T.K., Sherman, J., Fuller, D., Messing, E.M., Rubens, D.J., Strang, J.G., Brasacchio, R.A., Yu, Y., 2006. In-vivo measurement of surgical needle intervention parameters: a pilot study. *Conference proceedings : Annual International Conference of the IEEE Engineering in Medicine and Biology Society. IEEE Engineering in Medicine and Biology Society. Conference 1*, 3652-3655. doi: 10.1109/IEMBS.2006.259917

Simone, C., 2002. Modeling of needle insertion forces for percutaneous therapies. Department of Mechanical Engineering.

Surry, K., Austin, H., Fenster, A., Peters, T., 2004. Poly (vinyl alcohol) cryogel phantoms for use in ultrasound and MR imaging. *Physics in medicine and biology* 49, 5529. doi: 10.1088/0031-9155/49/24/009

van de Berg, N.J., Dankelman, J., van den Dobbelsteen, J.J., 2016. Endpoint Accuracy in Manual Control of a Steerable Needle. *Journal of vascular and interventional radiology : JVIR*. doi: 10.1016/j.jvir.2016.07.018

Zell, K., Sperl, J.I., Vogel, M.W., Niessner, R., Haisch, C., 2007. Acoustical properties of selected tissue phantom materials for ultrasound imaging. *Physics in Medicine and Biology* 52, N475. doi: 10.1088/0031-9155/52/20/N02